Life Sciences 263 (2020) 118577

Contents lists available at ScienceDirect

Life Sciences

journal homepage: www.elsevier.com/locate/lifescie

Zonisamide ameliorates neuropathic pain partly by suppressing microglial activation in the spinal cord in a mouse model

Hiroyuki Koshimizu[a,b], Bisei Ohkawara[b,*], Hiroaki Nakashima[a,b], Kyotaro Ota[a,b], Shunsuke Kanbara[a,b], Taro Inoue[a,b], Hiroyuki Tomita[a,b], Akira Sayo[c,d], Sumiko Kiryu-Seo[d], Hiroyuki Konishi[d], Mikako Ito[b], Akio Masuda[b], Naoki Ishiguro[e], Shiro Imagama[a], Hiroshi Kiyama[d], Kinji Ohno[b]

[a] Department of Orthopedic Surgery, Nagoya University Graduate School of Medicine, Nagoya, Japan
[b] Division of Neurogenetics, Center for Neurological Diseases and Cancer, Nagoya University Graduate School of Medicine, Nagoya, Japan
[c] Department of Oral and Maxillofacial Surgery, Nagoya University Graduate School of Medicine, Nagoya, Japan
[d] Department of Functional Anatomy and Neuroscience, Nagoya University Graduate School of Medicine, Nagoya, Japan
[e] Aichi Developmental Disability Center, Nagoya, Japan

ARTICLE INFO

Keywords:
Zonisamide
Neuropathic pain
Allodynia
Inflammatory cytokines
Spinal microglial activation

ABSTRACT

Neuropathic pain is caused by a lesion or a functional impairment of the sensory nervous system and allodynia is one of the frequently observed symptoms in neuropathic pain. Allodynia represents abnormal pain due to a non-noxious stimulus that does not normally provoke pain. Cellular mechanisms underlying neuropathic pain remain mostly elusive, and partial pain relief can be achieved in a limited number of patients by antidepressants, anticonvulsants topical anesthetics, and others. Zonisamide (ZNS) is widely used as an anti-epileptic and anti-Parkinson's disease drug. A recent report shows that ZNS suppresses neuropathic pain associated with diabetes mellitus in a mouse model. We made a mouse model of neuropathic pain in the hindlimb by cutting the nerve at the intervertebral canal at lumbar level 4 (L4). At 28 days after nerve injury, ZNS ameliorated allodynic pain, and reduced the expression of inflammatory cytokines and the nerve injury-induced increase of Iba1-positive microglia in the spinal dorsal horn at L4. In BV2 microglial cells, ZNS reduced the number of lipopolysaccharide-induced amoeboid-shaped cells, representing activated microglia. These results suggest that ZNS is a potential therapeutic agent for neuropathic pain partly by suppressing microglia-mediated neuroinflammation.

1. Introduction

Neuropathic pain is represented by four clinical features. Allodynia is provoked by a non-noxious stimulus that does not usually provoke pain. Hyperalgesia represents augmented pain provoked by a noxious stimulus. Paresthesia is a spontaneous or evoked unpleasant sensation. Anesthesia is insensitivity to pain. Neuropathic pain is often caused by nerve injury resulting from trauma, diabetes mellitus, narrowing of the intervertebral canal, and infection [1]. Up to 7–8% of the European population are affected by neuropathic pain, and 5% of the population have moderate to severe symptoms [2,3]. Pregabalin and non-steroidal anti-inflammatory drugs are currently prescribed for neuropathic pain, but usually have limited effects in most cases and sometimes with adverse effects [4,5]. Only 40–60% of patients generally achieve partial relieve [6]. Although the cellular mechanisms underlying neuropathic pain remain mostly elusive, recent studies revealed that microglia, immunocompetent cells in the central nervous system (CNS), play an important role in eliciting neuropathic pain [7–10].

Zonisamide (ZNS) was developed to treat epilepsy [11], and later found to be effective for Parkinson's disease (PD) [12]. In the brain of a mouse model of PD, ZNS suppresses expressions of tumor necrosis factor alpha (TNFα), the catalytic subunit of nicotinamide-adenine dinucleotide phosphate, reduced form (NADPH) oxidase, $gp91^{phox}$, and a mouse-specific microglial marker (F4/80) to exert a neuroprotective

Abbreviations: BSA, bovine serum albumin; CNS, central nervous system; IRF5, interferon regulatory factor-5; IRF8, interferon regulatory factor-8; LPS, lipopolysaccharide; NADPH, nicotinamide-adenine dinucleotide phosphate, reduced form; NOS, nitric oxide synthase; PD, Parkinson's disease; PWT, paw withdrawal threshold; PBS, phosphate-buffered saline; ROS, reactive oxygen species; TNFα, tumor necrosis factor alpha; WT, wild type; ZNS, zonisamide

* Corresponding author at: Division of Neurogenetics, Center for Neurological Diseases and Cancer, Nagoya University Graduate School of Medicine, 65 Tsurumai, Showa-ku, Nagoya 466-8550, Japan.
E-mail address: biseiohkawara@med.nagoya-u.ac.jp (B. Ohkawara).

https://doi.org/10.1016/j.lfs.2020.118577
Received 10 July 2020; Received in revised form 26 September 2020; Accepted 3 October 2020
Available online 13 October 2020

role [13]. We previously reported that ZNS promoted neurite elongation in primary spinal motor neurons (SMNs) in mice, and improved motor functions in a mouse model of sciatic nerve autograft [14,15]. We also reported that ZNS showed a neuroprotective effect against oxidative stress in mouse primary SMNs [14,15]. Other groups similarly reported that ZNS exerted anti-hyperalgesic and anti-allodynic effects. First, ZNS suppressed neuropathic pain in mouse models [16,17] and rat models [16,17] of diabetes mellitus, as well as in mice with formalin-induced neuropathy [16,17]. Second, in the Seltzer model, which is the most commonly used animal model of neuropathic pain by ligation of the sciatic nerve [18], either intracerebroventricular or intrathecal injection of ZNS showed anti-hyperalgesic and anti-allodynic effects [19]. The anti-hyperalgesic effects of ZNS were likely to be accounted for by blocking of sodium channel [11], blocking of T-type calcium channel [11,20], scavenging of free radicals [21], and inhibition of nitric oxide synthase (NOS) [22]. However, the anti-hyperalgesic and anti-allodynic effects of ZNS in central nervous system (CNS) have not been analyzed at the cellular level.

The present study was aimed to investigate the effects of ZNS on allodynia using a mouse model of neuropathic pain by cutting the L4 spinal nerve at the intervertebral canal. Additionally, we evaluated the effects of ZNS using cultured microglia and cultured sensory neurons.

2. Materials and methods

2.1. L4 spinal nerve injury mouse model

All animal studies including the L4 spinal nerve injury were approved by the Animals Care and Use Committee of Nagoya University (#30156, #31158, and #20153), and were conducted in accordance with the relevant guidelines. Wild type (WT) male C57BL/6J mice were purchased from Japan SLC Inc. Mice at 12–14 weeks of age were anesthetized by 2.5% isoflurane gas (Fujifilm Wako Pure Chemical). We cut the L4 spinal nerve at the intervertebral canal according to previous reports [23–26]. Briefly, skin incision was made from the lumber (L) level 3 to the top bone of the sacral (S) level 1 in the left side of the spine using the iliac crest as a positional guide. The L4 spinal nerve root region was exposed by trimming adjacent tissues while keeping the L5 transverse process intact. The left L4 spinal nerve, which is located rostral to the L5 transverse process, was carefully held and cut by micro scissors, while any of the L4 spinal nerve segment was not removed. In this study, we orally administered 30 mg/Kg/day of ZNS, because this concentration ameliorated sciatic nerve injury [15] and cervical spondylotic myelopathy [27]. Thirty mg of ZNS, which was kindly provided by Sumitomo Dainippon Pharma Co., Ltd., Japan, was dissolved in 10 ml of 0.5% methylcellulose, and 30 mg/Kg/day ZNS were intragastrically administered using a sonde needle (Natsume Seisakusho Co., Ltd) once a day. Control mice were administered with 0.5% methylcellulose once a day after surgery.

2.2. Behavioral tests

Allodynic hypersensitivity was evaluated by von Frey test and Catwalk gait analysis once a week after surgery for 35 days and 28 days, respectively. Mechanical allodynia, which is defined as lowering of a mechanical pain threshold, was evaluated by von Frey test [28]. Briefly, mice were placed on the wire mesh and covered by an opaque box for at least 30 min to be acclimated to the environment. We stimulated the planter surface of left or right hindpaw with 0.02 to 0.2 g von Frey filaments, and evaluated withdrawal responses of the hindpaw to the noxious mechanical stimuli. The 50% paw withdrawal threshold (PWT) was calculated using the up-down methods [28] and was blindly analyzed in 7 ZNS(−) mice and 7 ZNS(+) mice. Gait analysis was performed using the Catwalk XT Ver. 9 automated system (Noldus Information Technology, Wageningen, Netherlands) [29] at 3 days before surgery and once a week after surgery for up to 28 days in 11 ZNS(−) mice and 10 ZNS(+) mice. Catwalk automatically analyzes the detailed walking features of mice. Briefly, the Catwalk system has a horizontal glass plate with a computer-operated video-recording equipment placed underneath the glass plate. The mouse traversed a walkway without any interruption, and six complete crossings per mouse were analyzed. We evaluated three features (the max contact max intensity, the duty cycle, and the stride length) with the Catwalk system. The duty cycle indicates a ratio (%) of the time when each paw is in contact with the glass plate in a single step cycle. As the walking features could not be controlled by a researcher, the Catwalk analysis was not blinded.

2.3. Immunohistochemistry of dorsal horn at the L4 level

A ~4-mm-thick segment of the dorsal horn region at the L4 level was isolated on day 28 after surgery in 3 ZNS(+) mice and 3 ZNS(−) mice, as previously described [30,31]. Briefly, mice were deeply anesthetized with isoflurane and transcardially perfused with Zamboni's fixative solution (0.1 M phosphate buffer containing 2% paraformaldehyde and 0.2% picric acid). Laminae and vertebral bodies were removed, and a ~4-mm thick segment of the spinal cord at the L4 level was isolated and post-fixed with the same fixative solution for 15–18 h at 4 °C. Following a treatment with 20% sucrose in 0.1 M phosphate buffer overnight at 4 °C, the segment was stored at −80 °C. Then, the frozen segment was embedded in Tissue-Tek OCT compound (FSC 22 Clear, Leica Biosystems, 3801480) and sectioned into 14-μm thick slices. After washed with phosphate-buffered saline (PBS) three times, the slices were treated with 0.1% Triton X-100 and 1% bovine serum albumin (BSA) in 0.01 M PBS for 60 min. The specimen was then immunostained with anti-Iba1 antibody (1:500, Wako, 016-26461) and horse anti-mouse IgG antibody (1:1000, Funakoshi, FI-2000), and was observed under the BZ-X710 microscope (Keyence). The number of Iba1-stained cells that were positive for nuclear staining with Hoechst 33342 (Invitrogen, 3570) was quantified by two blinded observers using the BZ-X700 Analyzer BZ-H3A Ver. 1.31 (Keyence). The area of Iba1-positive signals was measured using the NIH Image J software (version 1.51j8).

2.4. Quantitative RT-PCR of the dorsal horn region at the L4 level

A ~4-mm-thick segment of the dorsal horn region at the L4 level was isolated on day 28 after surgery in 3 ZNS(+) mice and 3 ZNS(−) mice, as above. The samples were then subjected to total RNA extraction using QIAzol (Qiagen). First strand cDNA was synthesized with ReverTra Ace (Thermo Fisher). Quantitative RT-PCR was performed in duplicate using the SYBR Green I Master (Roche, 04707516001) and Light Cycler 480 (Roche). The expression level of each gene in the L4 dorsal horn region was normalized to that of *Gapdh*. The expression level of each gene in BV2 microglial cells was normalized to that of *B2m* encoding β2 microglobulin. Primer sequences are shown in Supplementary Table S1.

2.5. Culture of BV2 microglial cells and 50B11 sensory neuronal cells

BV2 cells were cultured in DMEM (Gibco, 11965-092) with 10% fetal bovine serum (Sigma, F7524) and 100 U/ml Penicillin-Streptomycin (Thermo Fisher, 15140-122) [32]. For the MTS assay, cells were seeded at 5.0×10^4 cells/well on a 96-well plate. After 24 h, cells were treated with 50 ng/ml lipopolysaccharide (LPS, Sigma, L2880-10MG) with variable concentrations of ZNS (0, 1, and 10 μM) for 24 h [33]. Then, cells were treated with MTS reagent (Promega, G3580) for 2 h to quantify MTS signals using a microplate reader (PowerScan HT, DS Pharma Biomaterial) according to the manufacturer's instructions. An MTS signal for each sample was normalized to that without ZNS or LPS treatment.

LPS treatment [34] activated BV2 microglia to be amoeboid-shaped along with enlargement of the cell body and reduction of ramification.

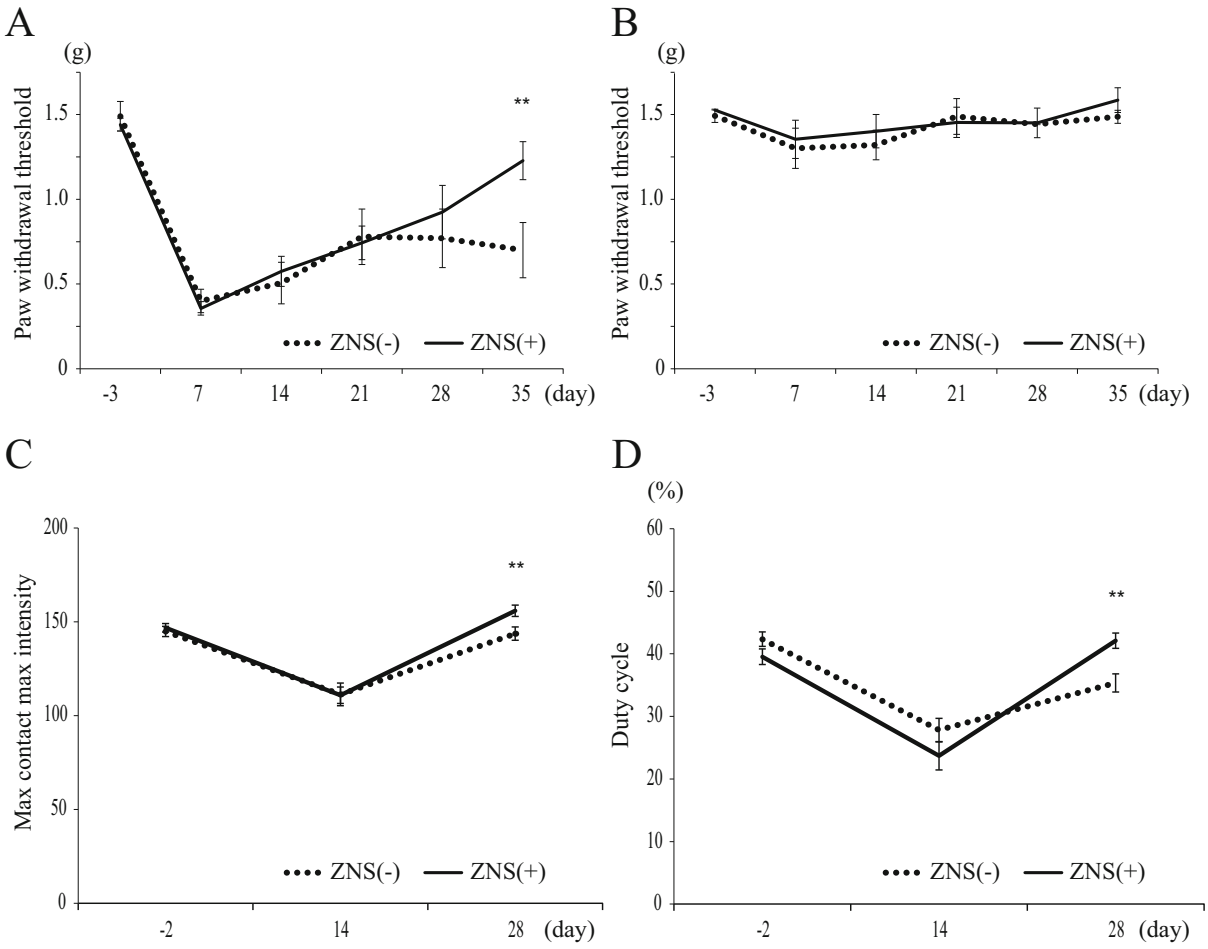

Fig. 1. ZNS ameliorates allodynia in a mouse model of neuropathic pain caused by L4 spinal nerve injury at the intervertebral canal.
(**A**, **B**) Paw withdrawal threshold (PWT) of ipsilateral (**A**) and contralateral (**B**) sides of control mice [ZNS(−)] and ZNS-administrated mice [ZNS(+)] before and after L4 spinal nerve injury ($n = 7$ mice each). The test was performed every week up to day 35 after surgery. (**C**, **D**) Catwalk gait analysis before and after L4 spinal nerve injury in 11 ZNS(−) mice and 10 ZNS(+) mice. The test was performed every other week up to day 28 after surgery. (**C**) The maximum intensity at maximum contact of the ipsilateral hindpaw in walking. (**D**) The duty cycle, which is the ratio of the ipsilateral hindpaw touching on a glass plate in a single walk cycle, was analyzed 6 times each. $^{**}p < 0.01$ by two-way repeated measured ANOVA followed by Tukey HSD. Mean and SE, not SD, are indicated.

Cell shape was observed by an Olympus IX71 microscope. For counting the number of amoeboid-shaped cells, BV2 microglia was seeded at 1.0×10^6 cells/well on a 6-well plate. Twenty-four hours after plating, cells were stimulated by addition of 50 ng/ml LPS with or without ZNS for 24 h. For quantitative RT-PCR, BV2 cells were cultured on a 6-well plate at 1.0×10^6 cells/well for 24 h, and then stimulated with 0.05 μg/ml LPS with or without ZNS for 2 h as previously described [35]. Total RNA was isolated using the QuickGene RNA cultured cell kit (Kurabo, RC-S) on QuickGene-800 (Kurabo).

2.6. Culture of 50B11 sensory neuron

An immortalized neuronal cell line derived from the rat dorsal root ganglion, 50B11, was kindly gifted from Dr. Ahmet Hoke at the Johns Hopkins University [36]. The 50B11 cells were cultured in Neurobasal medium (Gibco, 21103-049) or Neurobasal-A medium (Gibco, 10888022) including 10% fetal bovine serum (Sigma, F7524), 2% B27 supplement (Gibco, 17504-044), 0.2% glucose (Wako, 049-31165), and 0.5 mM L-glutamine (Gibco, 25030081) in a humidified atmosphere of 95% air-5% CO2 in a 37 ˚C incubator [36]. For immunostaining, cells were seeded at 1.0×10^4 cells/well on a 96-well plate coated with poly-L-lysine (Sigma, P8920) on day 1. Twenty-four hours after plating the cells, 75 μM forskolin (Tokyokasei, F0855) and 0, 1, 10, and 20 μM ZNS (Sumitomo Dainippon Pharma Co., Ltd., Japan) were added to the medium [15]. The cells were incubated for 48 h, and then fixed with 4% paraformaldehyde. Immunostaining was performed with anti-PGP9.5 antibody (1:700, GeneTex, GTX109637) followed by the horse FITC-conjugated anti-mouse antibody (1:400, Funakoshi, FI-2000) to stain neurites [37]. Cell nuclei were stained with Hoechst 33342 (Invitrogen, 3570). The number of Hoechst 33342-positive nuclei, as well as the length and the number of branch points of PGP9.5-positive neurites, in 9 fields per well were automatically quantified by the ArrayScan VTI HCS Reader (Thermo Scientific Cellomics). The number of nuclei, the neurite lengths, and the number of branch points were automatically analyzed by the Neuronal Profiling v4.0 BioApplication (Thermo Scientific Cellomics).

2.7. Statistical analysis

Data were analyzed by unpaired Student's *t*-test, Mann-Whitney *U* test, and one- or two-way ANOVA with post hoc Turkey HDS using the BellCurve add-ons for Excel (Social Survey Research Information). Student's *t*-test and one- or two-way ANOVA tests were applied after confirming that the data were distributed normally using Shapiro-Wilk test. Otherwise, Mann-Whitney *U* test was applied. Kruskal-Wallis test was not applied, because all multiply compared samples were distributed normally. *P* values of 0.05 or less were considered to be statistically significant.

3. Results

3.1. Zonisamide (ZNS) suppressed allodynia caused by the L4 spinal nerve injury

To evaluate the effect of ZNS on allodynia, we performed behavioral tests in a mouse model of neuropathic pain generated by cutting the L4 spinal nerve at the intervertebral canal. As has been reported by us [37] and others [23], this model exhibited no motor paralysis ($p > 0.05$, $n = 6$ mice each, Supplementary Fig. S1A). The amount of ZNS was 30 mg/Kg/day, which was three times higher than a dose adjusted for body surface area of the conventional human dose. This amount of ZNS ameliorated motor dysfunctions in rodent models of cervical spondylotic myelopathy [27] and sciatic nerve injury [14,15]. On the ipsilateral side of ZNS(−) mice, PWT was markedly decreased on day 7 after surgery, and was partially recovered up to day 21 (Fig. 1A). In contrast, ZNS enhanced the recovery of PWT up to day 35, although PTW did not return to the normal level. Statistical significance was observed on day 35 ($p < 0.001$, $n = 7$ mice each). PWT was not decreased on the contralateral side, and ZNS had no effect on PWT (Fig. 1B).

We next evaluated gait impairment due to neuropathic pain using the Catwalk system in 11 ZNS(−) mice and 10 ZNS(+) mice. An increase in the maximum intensity at maximum contact of hindpaws during walking in Catwalk is negatively correlated with mechanical allodynia [29]. The maximum intensity at maximum contact of the ipsilateral hindpaw was decreased on day 14, and ZNS had no effect (Fig. 1C). On day 28, however, the intensity was recovered almost to the normal level, and ZNS marginally but significantly enhanced the recovery ($p < 0.001$). The duty cycle indicates a ratio (%) of the time when each paw is in contact with the glass plate in a single step cycle, and is decreased after surgery due to refusal of stepping with a painful paw. The duty cycle of the ipsilateral paws was decreased on day 14, and ZNS had no significant effect (Fig. 1D). On day 28, however, the duty cycle was recovered better in ZNS(+) mice than that ZNS(−) mice ($p < 0.001$). These results suggested that daily ZNS administration for 35 days reduced allodynic pain and improved gait disturbance in a mouse model of neuropathic pain.

3.2. Zonisamide (ZNS) reduced the size of microglia in the ipsilateral dorsal horn in a mouse model of neuropathic pain

After peripheral nerve injury, microglia in the ipsilateral dorsal horn transforms from the resting state to the activated phenotype [38]. Then the activated microglia produces inflammatory cytokines that exacerbate neuropathic pain [39]. Iba1-positive microglia in the dorsal horn is increased in a mouse model of the L4 spinal nerve injury [39]. Immunostaining for Iba1 on day 28 showed that the L4 spinal nerve injury caused gathering of microglia in the spinal dorsal horn region, and ZNS treatment markedly reduced the size of Iba1-positive microglia in the ipsilateral dorsal horn ($p = 0.034$, $n = 3$ mice each, Fig. 2). These results suggested that ZNS suppressed the activation of microglia in the L4 dorsal horn in the mouse model.

3.3. Zonisamide (ZNS) downregulated expressions of genes encoding microglial activation and inflammatory cytokines in the ipsilateral dorsal horn in a mouse model of neuropathic pain

We examined gene expressions of *Cybb* (the catalytic subunit of NADPH oxidase, $gp91^{phox}$), *Tnf* (TNFα), and *Adgre1* (adhesion G protein-coupled receptor E1, F4/80). Expression of $gp91^{phox}$ is increased in activated microglia of the post-mortem brain in PD patients [40]. NADPH oxidase, which is composed of the $p91^{phox}$, $p22^{phox}$, $p47^{phox}$, $p67^{phox}$ and $p40^{phox}$ subunits [41], catalyzes the conversion of oxygen to superoxide (O_2^-), which in turn increases production of reactive oxygen species (ROS) [40]. TNFα is a cytokine, which induces an inflammatory response in CNS. F4/80 is a mouse-specific microglial marker. ZNS decreases the expression of $gp91^{phox}$ in the basal ganglia of PD mouse [13]. We found that ZNS downregulated gene expression of *Cybb* ($p = 0.017$, $n = 3$ mice each, Fig. 3) on day 28 after the L4 spinal nerve injury.

We additionally examined gene expressions of *Cd86* and *Cd68*, markers for activated M1 microglia; *Irf5* encoding interferon regulatory factor-5; *Itf8* encoding interferon regulatory factor-8; *P2x4r* encoding P2X4 receptor; and *Bdnf* encoding brain-derived neurotrophic factor [24–26,42]; as well as *Il1b* encoding interleukin 1β. We found that ZNS suppressed *Cd68* ($p = 0.027$), *Irf5* ($p = 0.005$), *Irf8* ($p = 0.001$), and *Il1b* ($p = 0.012$) ($n = 3$ mice each, Fig. 3). These findings suggested that ZNS suppressed expressions of some microglial activation markers and inflammatory cytokines with or without statistical significance.

3.4. Zonisamide (ZNS) suppressed LPS-induced activation of BV2 microglial cells

To confirm the effect of ZNS on suppression of microglial cells, we used BV2 microglial cells, which are immortalized by retroviral infection of a v-raf/v-myc oncogene and retain responsiveness to LPS [43]. We first confirmed that ZNS had no effect on proliferation of BV2 microglia in the presence of 0.05 μg/ml LPS ($p = 0.706$) (Fig. 4A). We next examined the effect of ZNS on the number of activated BV2 microglia. The number of amoeboid-shaped BV2 microglia after LPS stimulation was reduced by ZNS in a concentration-dependent manner ($p < 0.001$, a total 18 visual fields in 3 wells each, Fig. 4BC). Additionally, ZNS downregulated expressions of *Cybb* ($p < 0.001$), *Tnf* ($p < 0.001$), and *Adgre1* ($p < 0.001$) in BV2 microglia (a total 18 visual fields in 3 wells each, Supplementary Fig. S1BCD). These results suggested that ZNS suppressed activation of microglia and microglia-mediated inflammatory responses.

3.5. Zonisamide (ZNS) enhanced neurite elongation in 50B11 sensory neurons

We previously reported that the effects of ZNS on the enhancement of neurite elongation of primary spinal motor neurons and NSC34 cells, a hybrid cell line of neuroblastoma and spinal motor neuron, was maximized at 10 μM [15]. We here evaluated the neurite elongation of the 50B11 immortalized neuronal cell line derived from dorsal root ganglion to examine the effect of ZNS on the sensory nerve injury. After 48 h of ZNS treatment, cell viability, neurite length, and the number of branch points of neurites were measured in a blinded manner. We found that ZNS had no effect on cell viability ($p = 0.178$, more than 250 cells each) (Fig. 5A). ZNS, however, marginally increased the neurite length at 20 μM compared to those at 0 and 1 μM ($p < 0.001$, more than 250 cells each), and the number of branch points of neurites at 20 μM compared to that at 1 μM ($p = 0.014$, more than 250 cells each) (Fig. 5BC).

4. Discussion

Here, we found that ZNS, an anti-epileptic and anti-PD drug [13], exerted an anti-allodynic effect in a mouse model of neuropathic pain generated by cutting the L4 spinal nerve at the intervertebral canal (Fig. 1A–D). Lack of motor deficits in our mouse model (Supplementary Fig. S1A) suggested that ZNS had a direct effect on the sensory nervous system. Spinal nerve injury at the intervertebral canal activates microglia in the dorsal horn, which is substantiated by the changes in cell shapes and the proliferation of microglia [44], as well as by the upregulation of immune surface antigens and the production of inflammatory cytokines [45]. Activation of microglia in the dorsal horn is thus considered to be causally associated with the neuropathic pain. Microglia becomes activated in the spinal dorsal horn immediately after peripheral nerve injury [44]. Activated microglia express purinergic

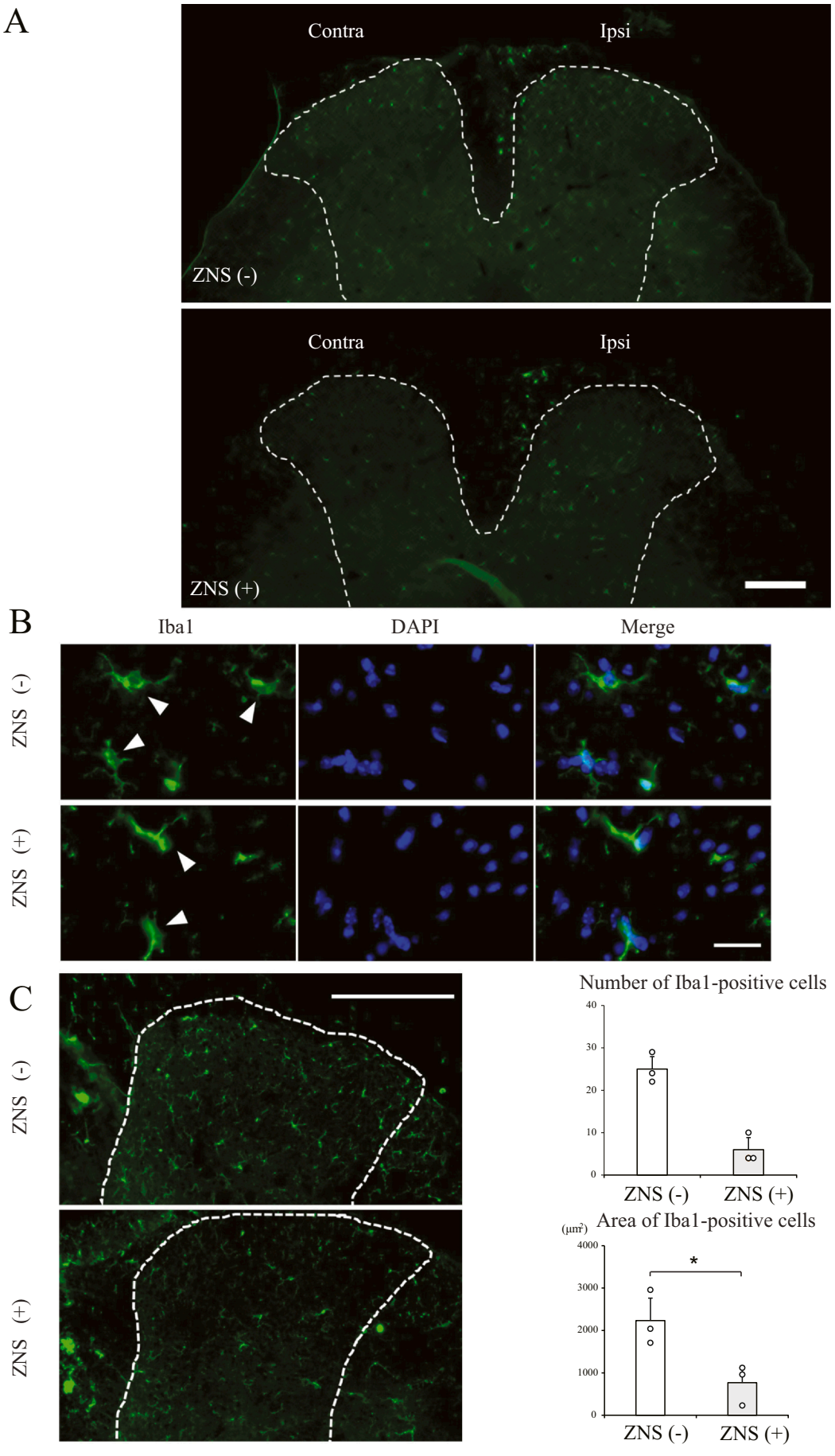

(caption on next page)

Fig. 2. ZNS suppresses the increased area of microglia in the ipsilateral dorsal horn region of the spinal cord in a mouse model of neuropathic pain.
(**A**) Ipsilateral (Ipsi) and contralateral (Contra) dorsal horns at the L4 level were stained with anti-Iba1 antibody on day 28 after L4 spinal nerve injury. Note scarce staining of Iba1 in the contralateral dorsal horn. Scale bar = 200 μm. (**B**) High magnification images of the ipsilateral dorsal horns. Scale bar = 20 μm. (**C**) Enlarged images of the ipsilateral dorsal horn, and quantification of the number and the area of Iba1-positive cells in the ipsilateral dorsal horn (n = 3 mice each). $^{*}p < 0.05$ by Mann-Whitney U test and Student's t-test. Mean and SD are indicated. Scale bar = 200 μm.

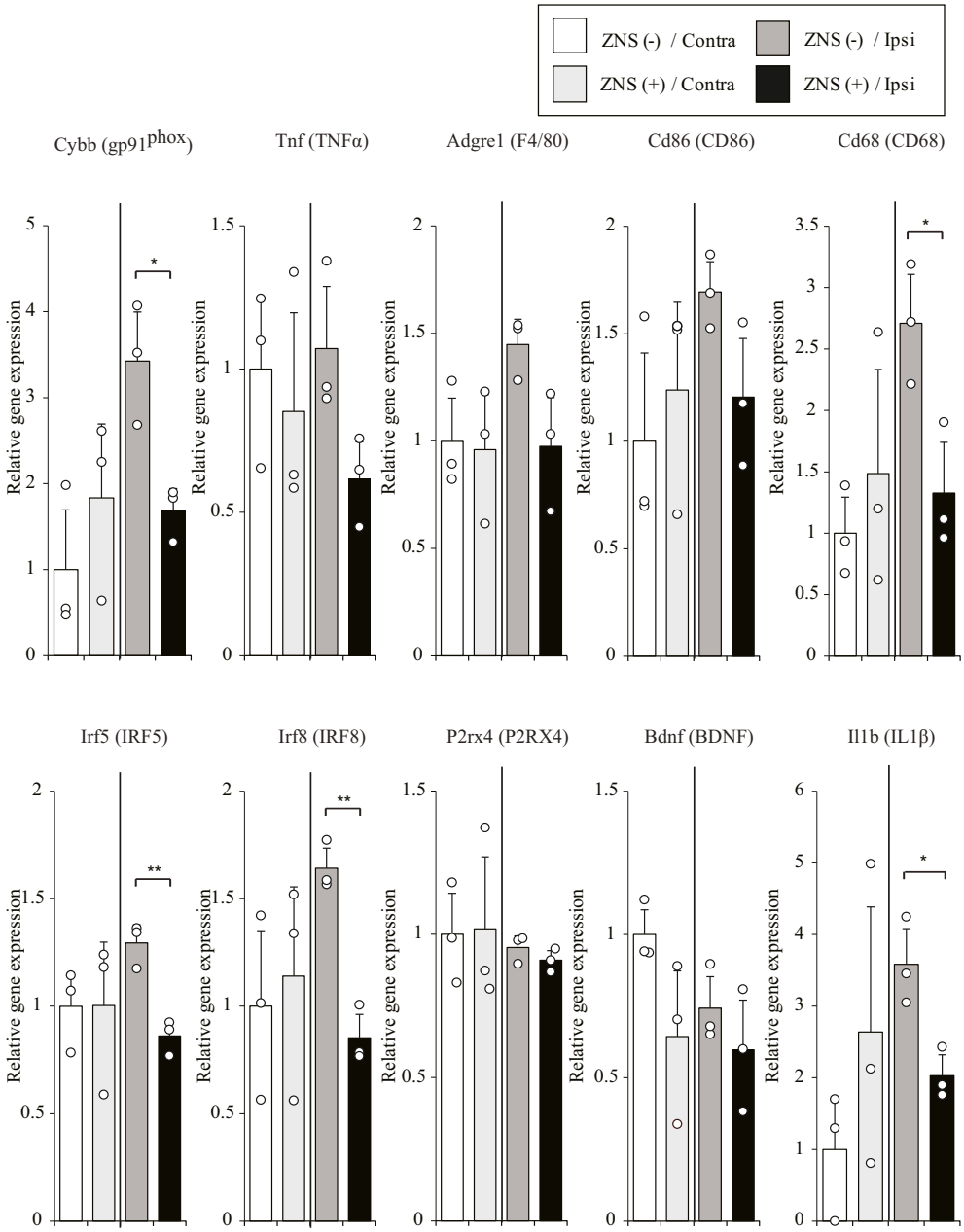

Fig. 3. ZNS suppresses mRNA expressions associated with microglial activation and proinflammatory responses.
Ipsilateral (Ipsi) and contralateral (Contra) L4 dorsal horn regions were harvested on day 28 after L4 spinal nerve injury (n = 3 mice each). Expressions of genes representing microglial activation and genes encoding proinflammatory cytokines were quantified by qRT-PCR. Gene expression was normalized for *Gapdh* and also for the ratio of contralateral ZNS(−) region. Mean and SD are indicated. $^{*}p < 0.05$ and $^{**}p < 0.01$ by student's t-test and Mann-Whitney U test. Mean and SD are indicated.

P2X4 receptor (*P2x4r*), brain derived neurotrophic factor (*Bdnf*), CD86 (*Cd86*), CD68 (*Cd68*), interferon regulatory factor-5 (*Irf5*), and interferon regulatory factor-8 (*Irf8*) [24–26,42]. Then microglia secrete inflammatory cytokines and reactive oxygen species (ROS) to contribute to the development and maintenance of pain hypersensitivity.

We observed that the increase of Iba1-positive microglia in the ipsilateral L4 dorsal horn was suppressed by ZNS (Fig. 2A–C). We also observed that the number of LPS-induced amoeboid-shaped BV2 microglia was decreased by ZNS (Fig. 4BC). ZNS suppressed gene expressions of *Cybb*, *Tnf*, and *Adgre1* in the dorsal horn at the L4 level in the mouse model (Fig. 3) and in cultured BV2 microglia (Supplementary Fig. S1BCD). Similar suppressions of gene expressions by ZNS were reported in the basal ganglia of a PD mouse model [13]. Previous report showed that ZNS exhibited analgesic effects against acute thermal and

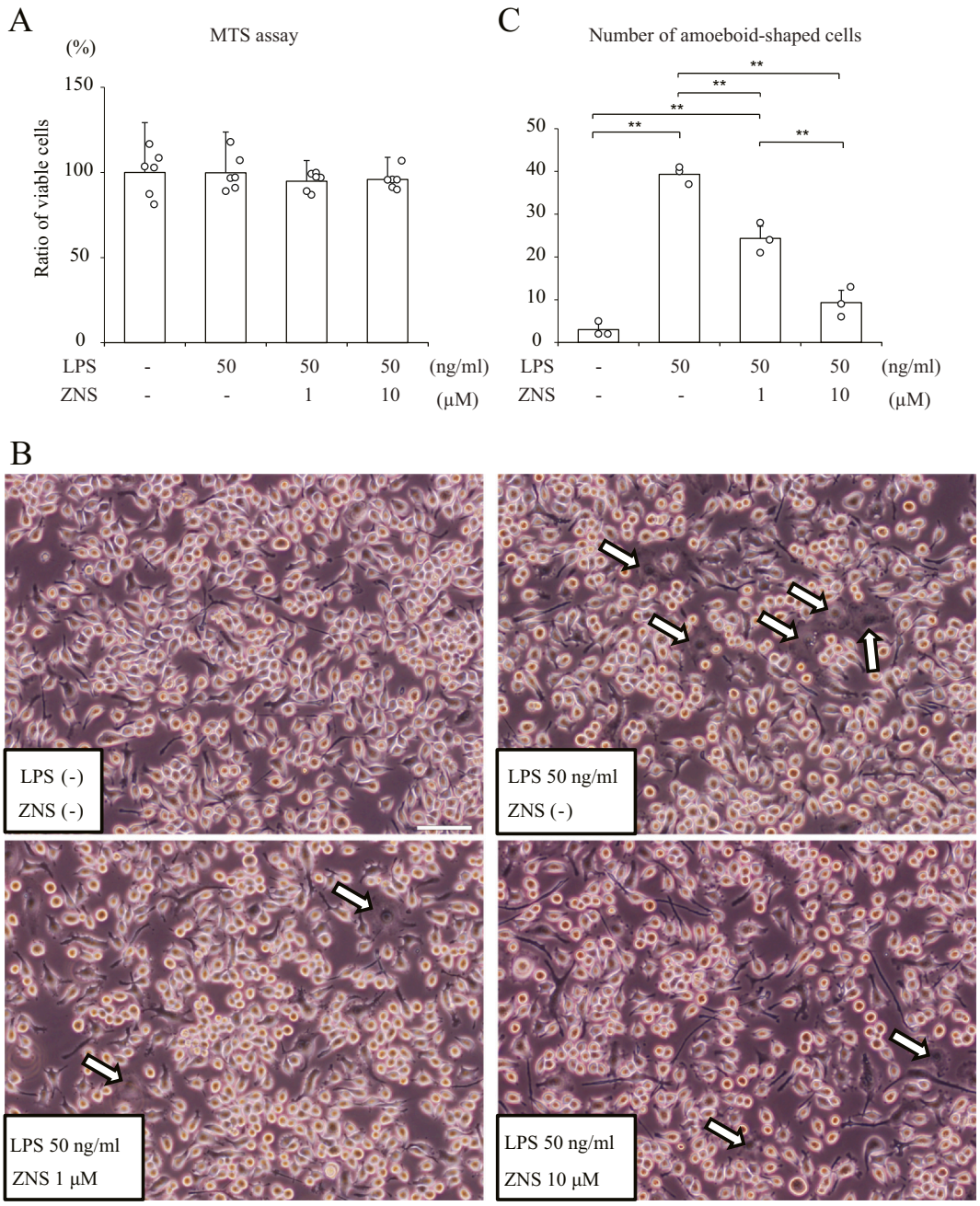

Fig. 4. ZNS suppresses LPS-induced morphological changes of BV2 microglial cells.
BV2 microglial cells were cultured with 0, 1, and 10 μM ZNS in the absence or presence of 50 ng/ml LPS for 24 h. (**A**) ZNS has no effect on the viability of BV2 microglial cells. The number of vial cells was measured by MTS assay, and was normalized for that without ZNS or LPS. (**B**) LPS induces enlargement of the cell body and amoeboid-shape transformation of BV2 cells (arrows). Scale Bar = 100 μm. (**C**) Quantification of the number of amoeboid-shaped cells in 6 fields per well ($n = 3$ wells each). $^{**}p < 0.01$ by one-way ANOVA followed by Tukey HSD. Mean and SD are indicated.

mechanical nociception [46]. In summary, ZNS is likely to have exerted an anti-neuropathic effect in part by suppressing a series of neuroinflammatory signaling events mediated by microglia in the dorsal horn. In addition, the blocking effects of ZNS on sodium channel [11] and T-type calcium channel [11,20] may also account for the anti-allodynic effect of ZNS. To make ZNS clinically available in the future, we need to perform additional studies to optimize the dosage and the administration protocols using animal models.

We previously reported that an anti-epileptic and anti-PD drug, zonisamide (ZNS), induces neurite elongation in primary spinal motor neurons (SMNs), and ameliorates motor deficits in a mouse model of sciatic nerve autograft [14,15]. In the study, we reported that ZNS increased the number of branch points and enhanced neurite elongation in primary spinal motor neurons and NSC34 cells. Here, ZNS also marginally increased the number of branch points, and enhanced neurite elongation of 50B11 cells (Fig. 5BC) without affecting the cell viability (Fig. 5A). Another group recently reported that ZNS enhanced neurite elongation in primary sensory neurons derived from the dorsal root ganglion [48]. On the other hand, another report shows that abnormal sprouting of injured primary afferent sensory nerves is linked to the pathobiology of peripheral neuropathic pain [47]. Thus, the neurite-elongating effect of ZNS on sensory neurons should have either an additive or adverse effect on the amelioration of neuropathic pain in our mouse model. Further mechanistic studies are required to prove the

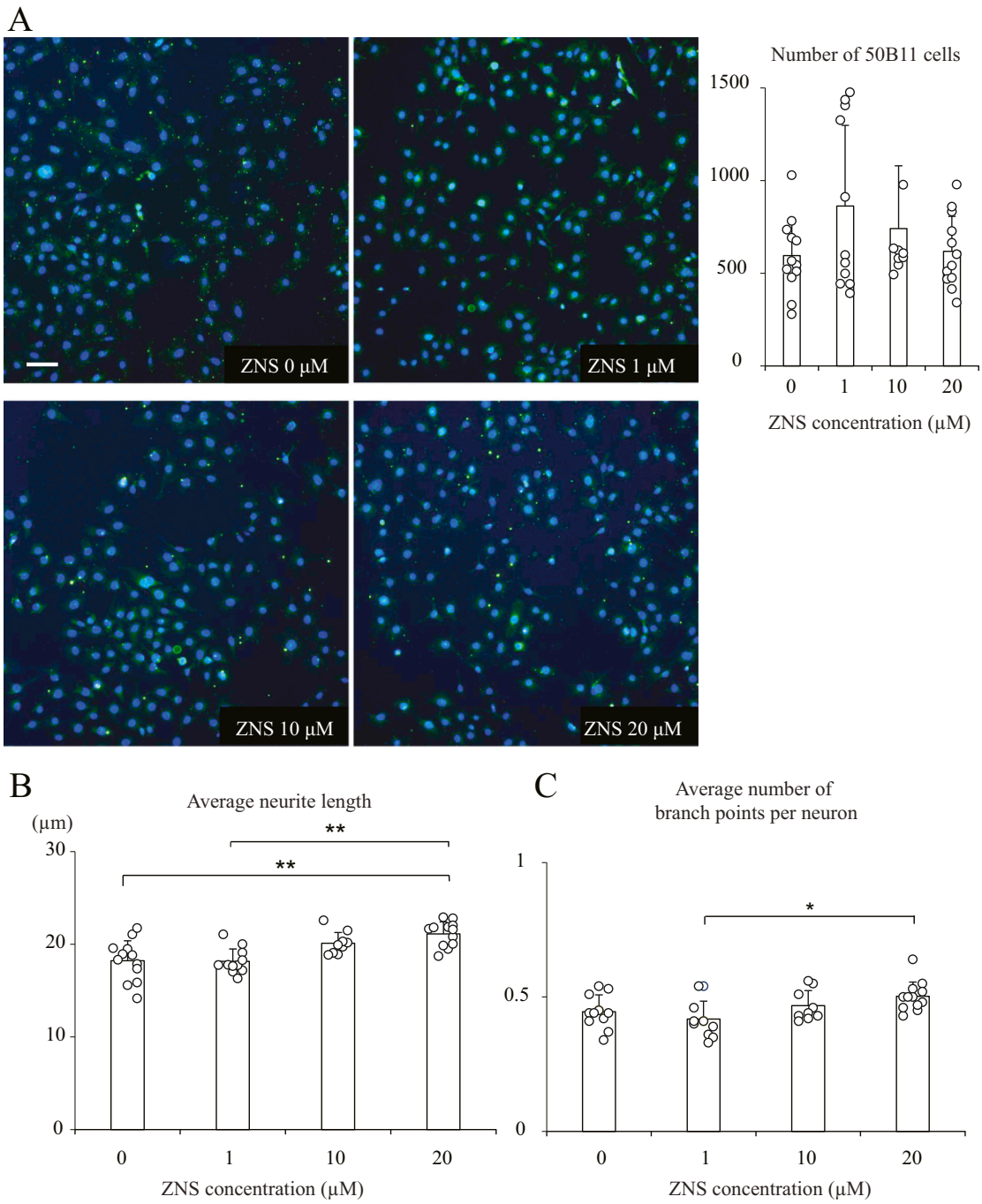

Fig. 5. ZNS increases the neurite length and the number of branch points in 50B11 cells.
The 50B11 immortalized rat sensory neurons were differentiated for 48 h in the presence of 0, 1, 10, and 20 μM ZNS. (**A**) The number of nuclei of 50B11 cells was automatically counted by ArrayScan. Scale Bar = 100 μm. (**B**) The neurite lengths in more than 250 cells were automatically measured by ArrayScan. (**C**) The number of branch points in more than 250 cells was automatically counted by ArrayScan. $^{*}p < 0.05$ and $^{**}p < 0.01$ by one-way ANOVA followed by Tukey HSD. No statistical difference in (**A**). Mean and SD are indicated.

neurite elongation effect of ZNS on neuropathic pain.

5. Conclusion

In this study, we found that Zonisamide (ZNS) suppresses allodynia in a mouse model of neuropathic pain. In the dorsal horn, ZNS reduces the expression of inflammatory cytokines and the number of nerve injury-induced microglia in the dorsal horn. Although additional studies are required to elucidate the molecular pharmacological mechanisms of ZNS and to prove the effect of ZNS in patients, we propose that ZNS potentially ameliorates neuropathic pain by at least in part suppressing microglia-mediated neuroinflammation.

Supplementary data to this article can be found online at https://doi.org/10.1016/j.lfs.2020.118577.

CRediT authorship contribution statement

Hiroyuki Koshimizu: Conceptualization, Validation, Formal analysis, Investigation, Data Curation, Writing - Original Draft, Writing - Review & Editing. Bisei Ohkawara: Conceptualization, Methodology,

Writing - Review & Editing, Project administration. Hiroaki Nakashima: Conceptualization, Writing - Review & Editing. Kyotaro Ota: Conceptualization. Shunsuke Kanbara: Conceptualization, Methodology. Taro Inoue: Formal analysis, Investigation. Hiroyuki Tomita: Investigation. Akira Sayo: Conceptualization, Methodology, Data Curation. Sumiko Kiryu-Seo: Conceptualization, Methodology. Hiroyuki Konishi: Conceptualization, Methodology, Funding acquisition. Mikako Ito: Conceptualization. Akio Masuda: Conceptualization. Naoki Ishiguro: Conceptualization, Funding acquisition. Shiro Imagama: Conceptualization, Methodology. Hiroshi Kiyama: Conceptualization, Funding acquisition. Kinji Ohno: Conceptualization, Methodology, Writing - Review & Editing, Funding acquisition, Supervision.

Declaration of competing interest

We declare no competing financial interests.

Acknowledgements

We would like to acknowledge Dr. Ahmet Hoke, Department of Neurology, School of Medicine, Johns Hopkins University for kindly providing us with 50B11 cells. We also would like to acknowledge Tomohiro Akashi, Ryusaku Esaki, Nobuaki Misawa, Kayo Yamaguchi, Harumi Kodama and Keiko Itano at Nagoya University for technical assistance, as well as Hisao Ishii and Kimitoshi Noto for making a mouse model. Zonisamide was kindly provided by Dainippon Sumitomo Pharma Co., Ltd. Japan.

Funding

This study was supported by Grants-in-Aids from the Japan Society for the Promotion of Science (JP18K06483, JP17K07094, JP18K06058, JP19K22802, and JP20H03561); the Ministry of Health, Labour and Welfare, Japan (H29-Nanchi-Ippan-030); the Japan Agency for Medical Research and Development (JP19gm1010002, JP19ek0109230, JP19ek0109281, and JP19bm0804005); and the Intramural Research Grant for Neurological and Psychiatric Disorders of NCNP (29-4).

References

[1] J.N. Campbell, R.A. Meyer, Mechanisms of neuropathic pain, Neuron 52 (1) (2006) 77–92.
[2] D. Bouhassira, et al., Prevalence of chronic pain with neuropathic characteristics in the general population, Pain 136 (3) (2008) 380–387.
[3] N. Torrance, et al., The epidemiology of chronic pain of predominantly neuropathic origin. Results from a general population survey, J. Pain 7 (4) (2006) 281–289.
[4] S. Mathieson, et al., Trial of pregabalin for acute and chronic sciatica, N. Engl. J. Med. 376 (12) (2017) 1111–1120.
[5] R.A. Moore, et al., Oral nonsteroidal anti-inflammatory drugs for neuropathic pain, Cochrane Database Syst. Rev. (10) (2015) Cd010902.
[6] R.H. Dworkin, et al., Pharmacologic management of neuropathic pain: evidence-based recommendations, Pain 132 (3) (2007) 237–251.
[7] D.E. Coyle, Partial peripheral nerve injury leads to activation of astroglia and microglia which parallels the development of allodynic behavior, Glia 23 (1) (1998) 75–83.
[8] K. Inoue, M. Tsuda, Microglia and neuropathic pain, Glia 57 (14) (2009) 1469–1479.
[9] M. Maeda, et al., Nerve injury-activated microglia engulf myelinated axons in a P2Y12 signaling-dependent manner in the dorsal horn, Glia 58 (15) (2010) 1838–1846.
[10] M. Yasui, et al., A chronic fatigue syndrome model demonstrates mechanical allodynia and muscular hyperalgesia via spinal microglial activation, Glia 62 (9) (2014) 1407–1417.
[11] Y. Masuda, et al., Zonisamide: pharmacology and clinical efficacy in epilepsy, CNS Drug. Rev. 4 (4) (1998) 341–360.
[12] M. Murata, Novel therapeutic effects of the anti-convulsant, zonisamide, on Parkinson's disease, Curr. Pharm. Des. 10 (6) (2004) 687–693.
[13] M.M. Hossain, et al., The anti-parkinsonian drug zonisamide reduces neuroinflammation: role of microglial Nav 1.6, Exp. Neurol. 308 (2018) 111–119.
[14] K. Ohno, et al., Repositioning again of zonisamide for nerve regeneration, Neural Regen. Res. 11 (4) (2016) 541–542.
[15] H. Yagi, et al., Zonisamide enhances neurite elongation of primary motor neurons and facilitates peripheral nerve regeneration in vitro and in a mouse model, PLoS One 10 (11) (2015) e0142786.
[16] N. Bektas, et al., Zonisamide: antihyperalgesic efficacy, the role of serotonergic receptors on efficacy in a rat model for painful diabetic neuropathy, Life Sci. 95 (1) (2014) 9–13.
[17] M. Tanabe, et al., Zonisamide suppresses pain symptoms of formalin-induced inflammatory and streptozotocin-induced diabetic neuropathy, J. Pharmacol. Sci. 107 (2) (2008) 213–220.
[18] Z. Seltzer, et al., A novel behavioral model of neuropathic pain disorders produced in rats by partial sciatic nerve injury, Pain 43 (2) (1990) 205–218.
[19] M. Tanabe, et al., Centrally mediated antihyperalgesic and antiallodynic effects of zonisamide following partial nerve injury in the mouse, Naunyn Schmiedeberg's Arch. Pharmacol. 372 (2) (2005) 107–114.
[20] S. Suzuki, et al., Zonisamide blocks T-type calcium channel in cultured neurons of rat cerebral cortex, Epilepsy Res. 12 (1) (1992) 21–27.
[21] A. Mori, et al., The anticonvulsant zonisamide scavenges free radicals, Epilepsy Res. 30 (2) (1998) 153–158.
[22] Y. Noda, et al., Zonisamide inhibits nitric oxide synthase activity induced by N-methyl-D-aspartate and buthionine sulfoximine in the rat hippocampus, Res. Commun. Mol. Pathol. Pharmacol. 105 (1–2) (1999) 23–33.
[23] S.H. Kim, J.M. Chung, An experimental model for peripheral neuropathy produced by segmental spinal nerve ligation in the rat, Pain 50 (3) (1992) 355–363.
[24] M. Tsuda, et al., P2X4 receptors induced in spinal microglia gate tactile allodynia after nerve injury, Nature 424 (6950) (2003) 778–783.
[25] T. Masuda, et al., IRF8 is a critical transcription factor for transforming microglia into a reactive phenotype, Cell Rep. 1 (4) (2012) 334–340.
[26] T. Masuda, et al., Transcription factor IRF5 drives P2X4R+-reactive microglia gating neuropathic pain, Nat. Commun. 5 (2014) 3771.
[27] S. Kanbara, et al., Zonisamide ameliorates progression of cervical spondylotic myelopathy in a rat model, Sci. Rep. 10 (1) (2020) 13138.
[28] S.R. Chaplan, et al., Quantitative assessment of tactile allodynia in the rat paw, J. Neurosci. Methods 53 (1) (1994) 55–63.
[29] D.H. Vrinten, F.F. Hamers, 'CatWalk' automated quantitative gait analysis as a novel method to assess mechanical allodynia in the rat; a comparison with von Frey testing, Pain 102 (1–2) (2003) 203–209.
[30] M. Kobayashi, et al., A DAP12-dependent signal promotes pro-inflammatory polarization in microglia following nerve injury and exacerbates degeneration of injured neurons, Glia 63 (6) (2015) 1073–1082.
[31] H. Konishi, et al., Annexin III implicated in the microglial response to motor nerve injury, Glia 53 (7) (2006) 723–732.
[32] Z. Yu, et al., Erianin inhibits high glucose-induced retinal angiogenesis via blocking ERK1/2-regulated HIF-1alpha-VEGF/VEGFR2 signaling pathway, Sci. Rep. 6 (2016) 34306.
[33] Q. Han, et al., 6-Shogaol attenuates LPS-induced inflammation in BV2 microglia cells by activating PPAR-γ, Oncotarget 8 (26) (2017) 42001–42006.
[34] C.U. Kloss, et al., Effect of lipopolysaccharide on the morphology and integrin immunoreactivity of ramified microglia in the mouse brain and in cell culture, Exp. Neurol. 168 (1) (2001) 32–46.
[35] W. Bi, et al., Rifampicin improves neuronal apoptosis in LPS-stimulated cocultured BV2 cells through inhibition of the TLR-4 pathway, Mol. Med. Rep. 10 (4) (2014) 1793–1799.
[36] W. Chen, et al., Immortalization and characterization of a nociceptive dorsal root ganglion sensory neuronal line, J. Peripher. Nerv. Syst. 12 (2) (2007) 121–130.
[37] A. Bhattacherjee, et al., Trophic factor and hormonal regulation of neurite outgrowth in sensory neuron-like 50B11 cells, Neurosci. Lett. 558 (2014) 120–125.
[38] M. Tsuda, et al., Neuropathic pain and spinal microglia: a big problem from molecules in "small" glia, Trends Neurosci. 28 (2) (2005) 101–107.
[39] M. Kobayashi, et al., TREM2/DAP12 signal elicits proinflammatory response in microglia and exacerbates neuropathic pain, J. Neurosci. 36 (43) (2016) 11138–11150.
[40] D.C. Wu, et al., NADPH oxidase mediates oxidative stress in the 1-methyl-4-phenyl-1,2,3,6-tetrahydropyridine model of Parkinson's disease, Proc. Natl. Acad. Sci. U. S. A. 100 (10) (2003) 6145–6150.
[41] B.M. Babior, NADPH oxidase: an update, Blood 93 (5) (1999) 1464–1476.
[42] K. Kobayashi, et al., Minocycline selectively inhibits M1 polarization of microglia, Cell Death Dis. 4 (3) (2013) e525–e.
[43] A. Henn, et al., The suitability of BV2 cells as alternative model system for primary microglia cultures or for animal experiments examining brain inflammation, Altex 26 (2) (2009) 83–94.
[44] K. Kohno, et al., Temporal kinetics of microgliosis in the spinal dorsal horn after peripheral nerve injury in rodents, Biol. Pharm. Bull. 41 (7) (2018) 1096–1102.
[45] M. Zhuo, et al., Neuronal and microglial mechanisms of neuropathic pain, Mol. Brain 4 (2011) 31.
[46] A. Sakaue, et al., Antinociceptive effects of sodium channel-blocking agents on acute pain in mice, J. Pharmacol. Sci. 95 (2) (2004) 181–188.
[47] A.J. Todd, A. Ribeiro-da-Silva, Anatomical Changes in the Spinal Dorsal Horn After Peripheral Nerve Injury//Zhuo M. Molecular Pain, Springer New York, New York, NY, 2007, pp. 309–324.
[48] S. Takaku, K. Sango, Zonisamide enhances neurite outgrowth from adult rat dorsal root ganglion neurons, but not proliferation or migration of Schwann cells, Histochem. Cell Biol. 153 (3) (2020) 177–184.